Influence of oxygen vacancies on the dielectric properties of hafnia: First-principles calculations

Eric Cockayne
Ceramics Division, Materials Science and Engineering Laboratory, National Institute of Standards and Technology, Gaithersburg, Maryland 20899-8520, USA

(Received 8 September 2006; revised manuscript received 13 January 2007; published 7 March 2007)

First-principles calculations were used to study the effects of neutral and 2+ charged oxygen vacancies on the dielectric properties of crystalline HfO_2. In agreement with previous results, the neutral vacancy is more stable on four fold-coordinated site, while the charged vacancy is more stable on a three fold-coordinated site. For both vacancy positions, HfO_2 remains insulating whether the vacancy is neutral or in the 2+ charge state. The dynamical matrix, Born effective charges, and electronic dielectric tensor were calculated for each structure. With one oxygen vacancy per 64 oxygen atoms, the static dielectric constant κ_s is increased by 1%–2% for neutral vacancies and suppressed by 1%–3% for 2+ charged vacancies, with the larger changes for three fold-coordinated vacancies. The exact result in the case of a charged vacancy depends on how the neutralizing charge necessary for macroscopic charge neutrality is modeled. The increase in κ_s for neutral oxygen vacancies arises from an enhancement of the electronic dielectric response due to a pair of electrons occupying an easily polarizable *F*-center defect state. The suppression in κ_s for charged oxygen vacancies is due to phonon hardening, which reduces the ionic response. No evidence is found for characteristic localized phonons induced by oxygen vacancies that could be detected by infrared or Raman spectroscopy.

DOI: 10.1103/PhysRevB.75.094103 PACS number(s): 63.20.Mt, 77.22.Ch, 77.84.Bw, 61.72.Ji

I. INTRODUCTION

The properties of HfO_2, including the fact that it has a higher static dielectric permittivity κ_s than SiO_2, make it one of the leading candidates for an alternate gate dielectric material.[1–3] One disadvantage of HfO_2 is that HfO_2 films exhibit an unstable threshold potential,[4] generally attributed to charge trapping. Defects, in particular, oxygen vacancies, have been considered as a likely source for such charge trapping.[4,5]

Many first-principles (FP) electronic calculations have been performed to better understand how defects affect the stability, crystal structure, and electronic structure of HfO_2. Earlier works[6–8] demonstrated that the electron levels associated with an oxygen vacancy lie within or near the Si band gap, and that charge states from 2+ to 0 (i.e., from zero to two electrons bound to the vacancy) are possible. Together, these results provide an explanation for how electrons from a Si substrate could become trapped or detrapped under operating conditions. Subsequent, more accurate, calculations[9–12] show that oxygen vacancies in HfO_2 can accommodate up to four electrons (charge states from 2+ to 2−, inclusive).[12]

It would be useful to quantify how much oxygen vacancies affect other properties of HfO_2, such as its phonon spectrum and dielectric permittivity, and how much these properties change when the charge state of the vacancy is changed. FP calculations have shown that the phonons and dielectric constant of crystalline HfO_2 can be reliably calculated,[13–15] but these works did not look at the effects of defects. In a recent paper,[16] Dutta *et al.* calculated the dielectric properties of the related material ZrO_2 with and without oxygen vacancies and found significantly softer phonon modes and a doubling of κ_s when oxygen vacancies were present. The concentration of O vacancies in their study was very large (12.5%), however, and they only considered the neutral defect charge state. In this work, the methodology used to calculate dielectric constants from FP is applied to the case of HfO_2 containing 1.6% oxygen vacancies to quantify the effect of oxygen vacancies on the phonon spectrum and dielectric properties. Two different O charge states are compared to investigate the effects of charge trapping on these properties.

The static dielectric tensor $\overleftrightarrow{\kappa}_s$ of a crystal can be written as $\overleftrightarrow{\kappa}_s = \overleftrightarrow{\kappa}_\infty + \overleftrightarrow{\kappa}_{ion}$, where $\overleftrightarrow{\kappa}_\infty$ is the electronic dielectric tensor and $\overleftrightarrow{\kappa}_{ion}$ the ionic contribution to the dielectric response. In turn, $\overleftrightarrow{\kappa}_{ion}$ can be written[17,18] as a sum of phonon contributions $(\overleftrightarrow{\kappa}_{ion})_\mu$,

$$\overleftrightarrow{\kappa}_{ion} = \sum_\mu (\overleftrightarrow{\kappa}_{ion})_\mu. \tag{1}$$

The components of $(\overleftrightarrow{\kappa}_{ion})_\mu$ are given in SI units by

$$(\kappa_{ion})_{\mu,\alpha\beta} = \frac{\overline{Z^\star_{\mu\alpha}}\,\overline{Z^\star_{\mu\beta}}}{V\epsilon_0 m_0 \omega_\mu^2}, \tag{2}$$

where ω_μ is the (angular) frequency of mode μ, V the volume per unit cell, and ϵ_0 the permittivity of free space. The individual components of the mode polarization vector for mode μ are given by

$$(\bar{Z}^\star_\mu)_\alpha \equiv \sum_{i\gamma} Z^\star_{i\alpha\gamma}(m_0/m_i)^{1/2}(a_\mu)_{i\gamma}, \tag{3}$$

where $Z^\star_i$ is the Born effective charge tensor for ion i, m_i its mass, $(a_\mu)_{i\gamma}$ the component of the normalized dynamical matrix eigenvector for mode μ involving ion i in the γ direction, and m_0 an arbitrary mass, which is canceled by the denominator of Eq. (2). In this work, scalar dielectric quantities such as κ_s are defined via

$$\kappa_s \equiv \frac{1}{3}\mathrm{Tr}\,\overleftrightarrow{\kappa}_s, \quad (4)$$

etc. From the above expressions, the effect of vacancies or other defects on the dielectric response of a material can be understood in terms of its effects on the phonon frequencies, ionic effective charges, etc.

II. METHODS

At room temperature, HfO_2 has a monoclinic unit cell with four Hf and eight O ions.[19,20] The oxygens occupy two crystallographically distinct sites: one with three fold Hf coordination and the other with four fold Hf coordination. The Hf occupy a single Wyckoff position with seven fold O coordination. The primitive 12-atom cell is too small for meaningful comparisons of different O vacancies. Instead, a 96-atom cell was used for the calculations, with each primitive lattice parameter doubled, as was done by Foster *et al.*[6] In total, five states were studied: defect-free HfO_2, labeled here "(0)," and the four states (3,0), (3,2+), (4,0), and (4,2+), where the first number refers to the coordination of the oxygen ion that was removed and the second number refers to the charge state.

Density-functional theory (DFT) electronic structure calculations for total energies, force constants, and Born effective charges were performed using the Vienna *ab initio* simulation package (VASP).[21] A plane-wave basis set was used for electronic wave functions. Projector augmented wave (PAW) pseudopotentials were used for Hf and O.[22,23] The Hf pseudopotential used has ten valence electrons ($5p$, $5d$, $6s$), while the O pseudopotential has six ($2s$, $2p$). The local-density approximation (LDA) was used for the exchange-correlation functional. In the study of Zhao and Vanderbilt,[13] the LDA was found to give better lattice parameters for HfO_2 than the alternate generalized gradient approximation (GGA) for the exchange-correlation functional, although a recent paper by Mukhopadhyay *et al.*,[24] using VASP PAW pseudopotentials, shows good agreement between the GGA lattice parameters and experiment. For calculation of the electronic contribution to the dielectric response, $\overleftrightarrow{\kappa}_\infty$, the DFT package ABINIT (Ref. 25) was used, with Hartwigsen-Goedecker-Hutter (HGH) pseudopotentials[26] and the LDA. The HGH Hf pseudopotential has 12 valence electrons ($5s$, $5p$, $5d$, $6s$); the O pseudopotential has six. The ABINIT code computes $\overleftrightarrow{\kappa}_\infty$ via the linear response to macroscopic electric fields within density-functional perturbation theory.[27]

Charges were controlled by adjusting the total number of electrons per unit cell (VASP) or the total cell charge (ABINIT). When the total ionic plus electronic charge per unit cell is not zero, a uniform compensating background charge is, in effect, incorporated so that the electrostatic energy converges (see, e.g, Ref. 28), but this background charge has no effect on the electronic structure or interatomic forces. The possibility of spin polarization was not investigated, as previous studies[6,12] have shown that the ground-state electronic configurations for the structures studied here are not spin polarized.

The structures studied were relaxed with a plane-wave cutoff energy of 337 eV and a $3\times3\times3$ Monkhorst-Pack k-point grid. For each state, the unit cell size and atomic positions were relaxed until the energy per HfO_2 formula unit was converged to 10^{-6} eV. Force constants were calculated via the frozen phonon method.[29] Each ion was displaced in turn by ±0.01 Å in each Cartesian direction, with the change in the Hellman-Feynman forces determining the corresponding row of the force constant matrix. Displacements of ±0.01 Å are large enough to determine the harmonic force constants accurately but small enough that the anharmonic force terms are negligible. The force constant matrix was then symmetrized to remove the remaining slight asymmetry, and a small correction was applied to the on-diagonal terms so that all of the rows and columns summed to zero. To reduce the computational burden associated with the force constant calculations, a cutoff energy of 250 eV and a $1\times1\times1$ Monkhorst-Pack grid were used. The Berry's phase method,[30,31] as encoded in the VASP software by Marsman, was used to calculate polarization changes as the ions were moved; from this method effective ionic charges Z^* could be determined. Berry's phase calculations each had one k point in the plane perpendicular to the polarization direction and three k points along the polarization direction. The electronic dielectric tensor $\overleftrightarrow{\kappa}_\infty$ was computed for a primitive defect-free HfO_2 cell using k-point grids of different sizes and different plane-wave cutoff energies. The results were then extrapolated to the infinite cutoff, infinite k-point grid limit. The $\overleftrightarrow{\kappa}_\infty$ for the defect supercells were estimated by calculating $\overleftrightarrow{\kappa}_\infty$ using one k point and a series of cutoff energy up to 385 eV. The ratios of these values to those for a defect-free cell with the same k-point grid and cutoff energy were determined, and the extrapolated ratios were then applied to the extrapolated estimate of $\overleftrightarrow{\kappa}_\infty$ for defect-free HfO_2.

The error in the results for the large unit cell calculations due to the choice of cutoff energies, finite k-point grids, and extrapolation methods was estimated from test calculations on 12-atom HfO_2 cells as a function of cutoff energy, etc., and determined to be ±5 cm^{-1} for phonon frequencies, ±0.01 for effective charges, and ±0.05 for the elements of κ_∞.

III. RESULTS

A. Electronic structure and energy

The electronic density of states of the neutral (3,0) structure is shown in Fig. 1. Removing one O from HfO_2 results in a structure where the sum of the nominal ionic charges (Hf 4+; O 2−) is 2+. The two "excess" electrons in the charge neutral cell do not fill empty conduction band states to make the system metallic; rather they localize in a midgap defect state[6,9] localized at the vacancy site (Fig. 1) to form an F center. Removing these two electrons yields a 2+ charged state where the highest occupied states correspond to the top of the O $2p$ band. In both cases, there is a gap between the highest occupied and lowest unoccupied states; thus the system is insulating and the electronic contribution to $\overleftrightarrow{\kappa}_s$ is nonsingular (unlike the case for a metal). The calculated band gaps are 4.1 eV for (0), and the calculated energy difference between the defect states and the conduction band are 1.6 eV for (4,0) and 1.2 eV for (3,0). These results include substantial local DFT errors. More sophisticated electronic structure

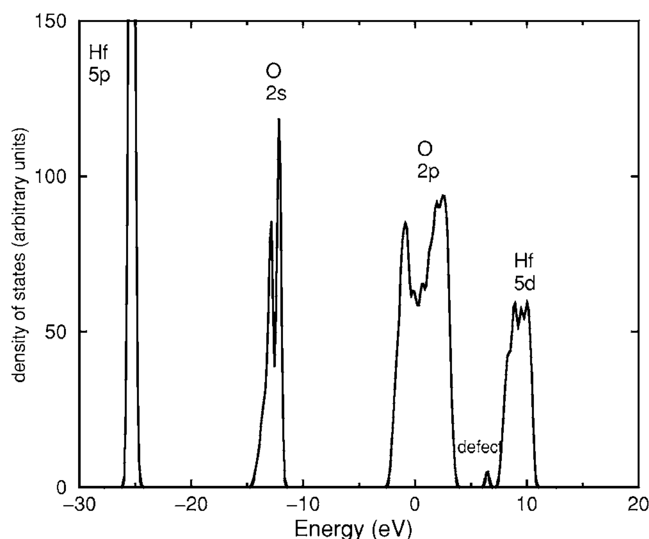

FIG. 1. Electronic density of states for HfO_2 and for HfO_2 with a neutral O vacancy in the three coordinated position. Primary character of bands indicated.

calculations[9,12] yield corresponding band gaps about 50% larger, placing the band gap for defect-free HfO_2 close to its experimental value of 5.7 eV,[32] and place the neutral vacancy states 1.9 eV below the conduction band for metastable tetragonal HfO_2 (Ref. 9) and 3.2 eV below the conduction band for monoclinic HfO_2.[12]

B. Relaxation and energetics

The relaxed cell parameters are shown in Table I. The calculated cell is smaller than the experimental one, as is typical for LDA calculations, but the calculated positional parameters for (0) (not shown) are all within 0.005 of the corresponding experimental values. Although the Hf nearest the 2+ charged vacancies are farther from the vacancy on average than the Hf nearest the neutral vacancies, as can be understood from electrostatic repulsion between like charges, the charged vacancies have smaller unit cells than the neutral ones. Note that the cell relaxations in Table I correspond to a 1.6% oxygen vacancy concentration. Due to interactions between vacancies, the change in volume per vacancy may differ from that of an isolated vacancy.

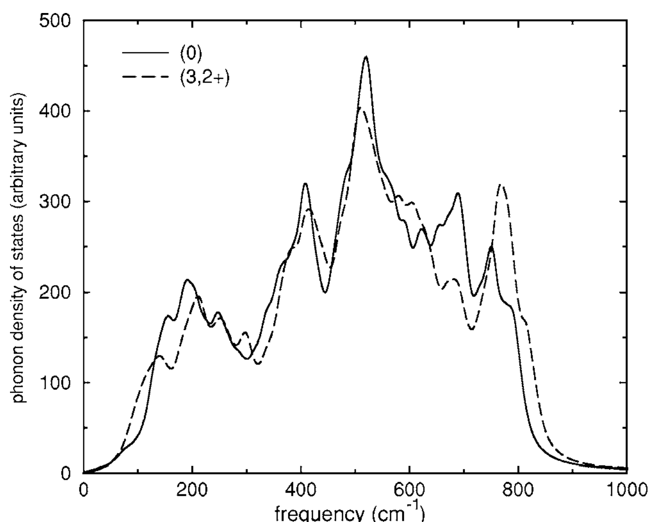

FIG. 2. Calculated phonon density of states in (0) and (3,2+).

For the fully relaxed structures, (4,0) was 0.09 eV lower in energy than (3,0), but (3,2+) was 0.81 eV lower in energy than (4,2+). These results are in excellent agreement with those of Foster *et al.*,[6] who found (4,0) 0.02 eV lower in energy than (3,0) and (3,2+) 0.76 eV lower in energy than (4,2+).

C. Phonons, effective charges, and dielectric response

Each defect structure has $N=95$ atoms and therefore $3N-3=282$ optical phonons. Phonon spectra are shown in Fig. 2. The results are very similar for all the defect states, so only the results for defect-free HfO_2 and for (3,2+) are shown. Each individual mode has been given a Lorentzian broadening with a broadening parameter of 30 cm^{-1} to smooth the data [see Eq. (5) below]. Overall, the presence of an O vacancy leads to some hardening of the phonons, especially around 750 cm^{-1}. In contrast to the case for the electronic density of states, the addition of an O vacancy does not lead to any localized vibrational modes. The individual zone-center phonon frequencies calculated for defect-free monoclinic HfO_2 are shown in Table II. They are generally intermediate in frequency between the LDA and the GGA results of Zhao and Vanderbilt.[13] The calculated Raman fre-

TABLE I. Comparative crystallographic parameters for the relaxed structures (a, b, and c scaled by 0.5 and V by 0.125 for comparison with the primitive cell). Lattice parameters are in Å, angles in degrees, and volumes V in Å^3. Experimental data are from Refs. 19 and 20.

Structure	a	b	c	α	β	γ	V
0	5.032	5.124	5.194	90	99.53	90	132.10
(4,2+)	5.007	5.126	5.134	90.23	99.06	89.97	130.16
(4,0)	5.028	5.128	5.181	90.03	99.45	90.00	131.78
(3,2+)	5.013	5.112	5.156	90.01	99.25	90.21	130.42
(3,0)	5.027	5.123	5.189	90.05	99.45	89.96	131.84
Expt.	5.117	5.175	5.291	90	99.22	90	138.32

TABLE II. Calculated phonon frequencies for monoclinic HfO_2. For infrared-active transverse optical (IR) and for longitudinal optical (LO) modes, starred frequencies are those predicted to be most easily observed experimentally, while the superscript *s* denotes a peak that might be observed as a shoulder to the intense peak of closest frequency. Symmetries are given for the Raman and IR-active modes.

Raman		IR		LO	
A_g	B_g	A_u	B_u		
129	138	140	247^*	140	421
141	173	188	259^s	188	493^*
153	248	265^s	334^*	252	521
261	339	373^*	355^s	259	603^*
355	413	424^s	417^*	275^*	670
398	526	514^s	530^*	346	679^*
503	568	627^*	753^*	363	795^*
590	649	672		393^*	
687	790				

quencies are generally about 10 cm^{-1} higher than the experimentally measured ones,[33] and the calculated infrared frequencies are on average about 15 cm^{-1} higher than the experimental ones.[34]

The formula for the static dielectric response is given in Sec. I. The frequency-dependent complex dielectric function is estimated via a damped oscillator model, with the $(\kappa_{ion})_\mu$ of Sec. I replaced by

$$(\kappa_{ion})_\mu(\omega) = \frac{(\kappa_{ion})_\mu \omega_\mu^2}{\omega_\mu^2 - \omega^2 - i\omega\gamma_\mu}. \quad (5)$$

The damping parameters γ_μ cannot readily be calculated from first principles. Instead, the typical width of the spectral features of experimental data[35] have been used to obtain a simple estimate of $\gamma_\mu \approx 30$ cm^{-1} for all modes.

The Born effective charges found for defect-free HfO_2 (Table III) are similar to previous results,[13] but about 3% smaller. In HfO_2 with defects, the Born effective charges are similar in the bulk, but suppressed near the vacancy as discussed in Sec. IV. The sum of the Born effective charges was 0 for the neutral cells and +2 for the 2+ charged cells. The lack of (ionic plus electronic) neutrality has implications for the dielectric properties. If the compensating background charge is treated as spatially fixed and inert except for electrostatic interactions with the medium, then there is an acoustic contribution to the frequency-dependent dielectric response;

$$\frac{Z^2}{V\epsilon_0 M}\frac{1}{(-\omega^2 - i\omega\gamma_A)}, \quad (6)$$

where Z is the total (nuclear plus electronic, but not compensating background) charge per unit cell, M the total mass, and γ_A an acoustic damping factor. This term leads to a divergence in κ_s, corresponding to the ions moving under an applied static electric field while the background charge remains fixed.

The above approximation, however, is unphysical. The compensating charge in a real system is not inert. A proper dielectric calculation would explicitly include the source of the compensating charge, i.e., defects of opposite charge to those included and calculate the lattice dynamics and effective charges in a system containing both kinds of defects. Such an approach is beyond the scope of this paper. Instead, the effect of the compensating defects has been treated by simply modifying the Born effective charges so that the on-diagonal components become

$$Z^{\star\prime}_{i\alpha\alpha} = Z^{\star}_{i\alpha\alpha} - \frac{Z}{N}. \quad (7)$$

An argument for this approximation is as follows. Suppose that the +2 charge of each charged oxygen vacancy is compensated by a negatively charged interstitial. Suppose that these interstitials are bonded to the existing atoms at random and move along with them, otherwise not affecting the lattice dynamics. Each compensating charge thus decreases the ef-

TABLE III. Calculated Born effective charge tensors for defect-free monoclinic HfO_2. O_1 and O_2 are three fold and four fold coordinated, respectively. The specific choice of ions match those of Ref. 13.

	xx	*xy*	*xz*	*yx*	*yy*	*yz*	*zx*	*zy*	*zz*
Hf	5.33	−0.39	0.22	−0.12	5.31	0.16	0.23	0.35	4.75
O_1	−2.94	1.01	−0.22	1.27	−2.58	−0.62	−0.19	−0.61	−2.22
O_2	−2.38	0.08	0.00	0.15	−2.74	0.34	−0.04	0.41	−2.53

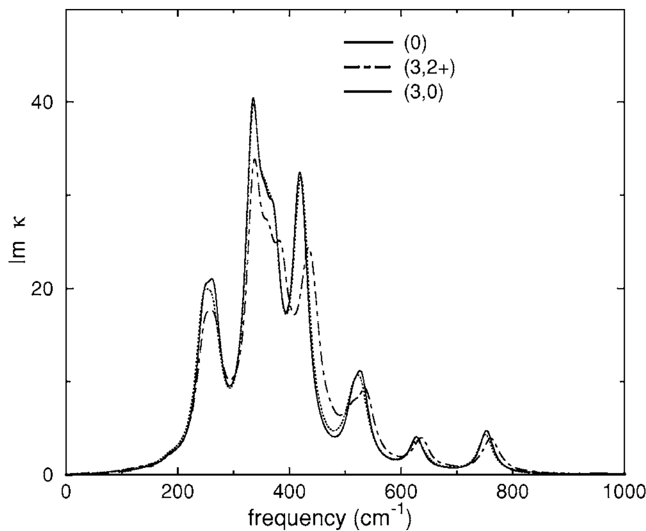

FIG. 3. Predicted Im $\kappa(\omega)$ of HfO_2 with and without oxygen vacancies, using phonon frequencies and optical strengths calculated from first principles and a damped oscillator model with a 30 cm^{-1} damping coefficient for all modes.

fective charge of the ion it is bound to by 2. Now, since the modes that contribute to the dielectric response are the zone-center (i.e., long wavelength) modes, we can take a crystallographic average of Born effective charges, without affecting the results. Equation (7) follows from the random distribution assumption. By replacing $\overleftrightarrow{Z}$ with $\overleftrightarrow{Z}'$, the singularity in κ_s is eliminated.

The dielectric functions as calculated from Eqs. (2), (3), (5), and (7) are shown in Figs. 3–5. The peaks for Im κ are the most intense IR-active transverse optical (TO) modes. The peaks for Im κ^{-1} show the most significant longitudinal optical (LO) modes. In the low-frequency limit, Re κ gives the static dielectric constant. Only the results for (0), (3,0), and (3,2+) are shown, as the results for (4,0) and (4,2+) are similar to those for (3,0) and (3,2+), respectively.

The highest-frequency phonons are of particular interest for infrared studies of thin-film gate dielectric materials.[36–39]

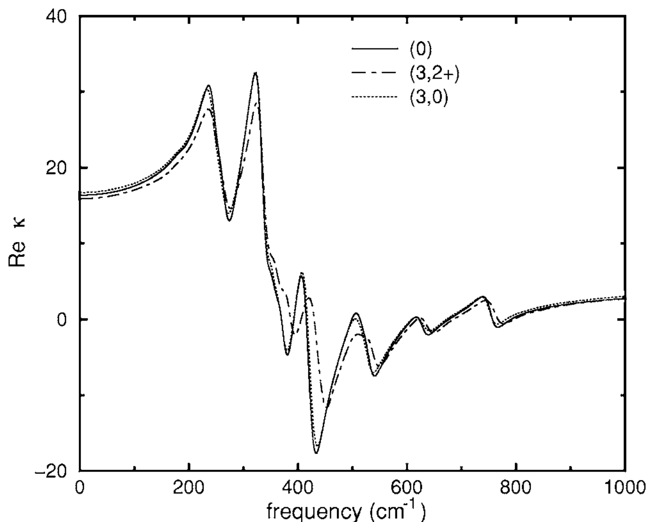

FIG. 4. Same as Fig. 3, but for Re κ.

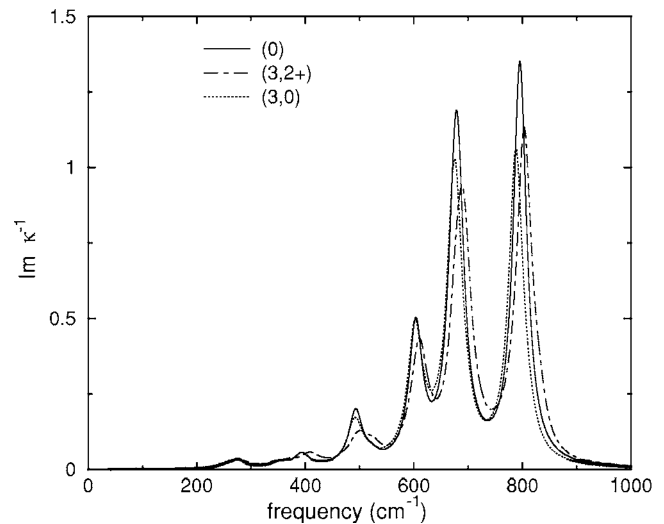

FIG. 5. Sames as Fig. 3, but for Im κ^{-1}.

In Table IV, the calculated frequencies of the highest-frequency TO and LO phonons are given for each structure. The results assume a polycrystalline sample, as the dielectric tensor has been averaged to obtain a scalar dielectric function [Eq. (4)].

No evidence is seen in Figs. 3–5 for any intense IR-active localized phonon introduced by an oxygen vacancy. A vacancy could very plausibly induce a local "breathing-type" phonon involving the surrounding ions; such a phonon, however, would be expected to be *Raman* active. Calculation of Raman intensities from first principles for such large cells is cumbersome; therefore, a crude estimate of Raman tensors was done as follows. The oxygen positions in the nearest-neighbor shell of each cation were calculated in equilibrium and then with a small amplitude displacement pattern of a specific phonon imposed. For each cation, the symmetric strain tensor was found that, when applied to the "before″ oxygen positions, gave the best least-squares fit to the "after" positions. The strain tensors for each cation were then added and used as a proxy for the Raman tensor for the chosen phonon. The procedure was repeated for all phonons. Comparison of the estimated Raman intensities of defect-free HfO_2 and the HfO_2 cell with oxygen vacancies did not show any evidence for local Raman-active modes induced by O vacancies.

The calculated $\overleftrightarrow{\kappa}_s$ for the various structures are given in Table V. The calculated ionic contribution to the dielectric

TABLE IV. Calculated frequencies of highest-frequency TO and LO phonons for each structure studied (in cm^{-1}). The values for the defect structures correspond to a 1.6% oxygen vacancy concentration and are expected to be concentration dependent.

Structure	TO	LO
(0)	753	795
(4,2+)	759	794
(4,0)	749	790
(3,2+)	760	803
(3,0)	751	787

TABLE V. Dielectric tensors and $\kappa=(\kappa_{11}+\kappa_{22}+\kappa_{33})/3$ for κ_{ion}, κ_∞, and κ_s for each structure. Values of 0 are exactly zero by symmetry.

Structure	response	κ_{xx}	κ_{xy}	κ_{xz}	κ_{yy}	κ_{yz}	κ_{zz}	κ
(0)	κ_∞	4.9	0	0.1	4.9	0	4.6	4.8
(4,2+)	κ_∞	4.9	0.0	0.1	4.9	0.0	4.6	4.8
(4,0)	κ_∞	5.1	0.0	0.1	5.1	0.0	4.8	5.0
(3,2+)	κ_∞	4.9	0.0	0.1	4.9	0.0	4.6	4.8
(3,0)	κ_∞	5.1	0.0	0.1	5.2	0.1	4.9	5.1
(0)	κ_{ion}	13.3	0	1.0	12.3	0	9.1	11.5
(0) (Ref. 13)	κ_{ion}	13.1	0.0	1.8	10.8	0.0	7.5	10.5
(4,2+)	κ_{ion}	13.2	−0.1	0.9	12.0	−0.1	8.8	11.3
(4,0)	κ_{ion}	13.3	0.0	1.1	12.2	0.0	8.9	11.5
(3,2+)	κ_{ion}	12.6	0.0	0.9	11.8	−0.2	8.9	11.1
(3,0)	κ_{ion}	13.6	0.0	0.9	12.3	0.1	9.0	11.6
(0)	κ_s	18.1	0	1.1	17.2	0	13.7	16.3
(4,2+)	κ_s	18.1	−0.1	1.1	16.9	−0.1	13.4	16.1
(4,0)	κ_s	18.4	0.0	1.2	17.3	0.0	13.7	16.5
(3,2+)	κ_s	17.4	0.0	1.0	16.7	−0.2	13.5	15.9
(3,0)	κ_s	18.7	0.0	1.0	17.5	0.1	13.9	16.7

response of defect-free HfO_2 is slightly larger than the one determined by Zhao and Vanderbilt.[13]

IV. DISCUSSION

The calculated dielectric constant for defect-free monoclinic HfO_2 of 16.3 is lower than the reported experimental value of 22 (Ref. 2). This discrepancy has been attributed to the possible presence of other HfO_2 phases of higher permittivity.[13] Another possible explanation is that the LDA lattice parameter underestimation leads to phonons that are too stiff and reduces the permittivity. A recalculation of the dielectric constant of HfO_2 at the experimental volume gives a value of 18.4. Thus, not all of the discrepancy can be explained by the LDA volume error. In any case, the relative trends due to defects are not expected to be affected by the volume error.

While the overall phonon density of states (DOS) is found to be changed by the introduction of vacancies, the changes in dielectric constant are relatively small (Table V): 3% or less with one O vacancy per 64 O atoms. The polar phonons that dominate the dielectric response of HfO_2 are thus relatively unaffected by the introduction of O vacancies. To the extent that vacancies do change κ_s, neutral vacancies tend to enhance the dielectric response and charged vacancies tend to suppress it. As seen in Table V, the enhancement of κ_s for the neutral vacancies mainly arises largely from increased κ_∞, while the suppression of κ_s for the charged vacancies is largely due to smaller ionic contribution to the response κ_{ion}. Detailed study of the structures and phonon properties show that the structures with neutral vacancies are relatively "rigid:" the atomic positions do not shift much with respect to the positions in the defect-free structure. Charged vacancies cause more significant structural relaxation because of electrostatic interactions. The structural relaxation in the case of charged defects leads to slightly increased phonon frequencies $\nu_\mu=\omega_\mu/(2\pi)$ for those phonons which contribute most to the dielectric response (Fig. 3), lowering the response, as individual polar mode contributions to the dielectric constant are proportional to $1/\omega^2$, all else being equal [Eq. (2)].[18] The enhancement of κ_∞ for the neutral vacancies arises from the electrons occupying the easily polarizable defect states. The small changes in κ_s in monoclinic HfO_2 introduced by oxygen vacancies are in contrast to the approximate doubling of κ_s calculated for a phase transformation to metastable cubic HfO_2.[13,40] This suggests that the calculated doubling of κ_s of the related compound ZrO_2 upon the introduction of 12.5% oxygen vacancies[16] is *not* primarily due to the oxygen vacancies themselves, but due to the stabilization of the cubic phase relative to the monoclinic phase.

The dielectric function sum rule,[41] in the case of an ionic crystal, can be written as

$$\sum_\mu \kappa_\mu \omega_\mu^2 = \frac{1}{V\epsilon_0}\sum_i \frac{(Z_i^\star)^2}{m_i}, \tag{8}$$

where

$$(Z_i^\star)^2 \equiv \frac{1}{3}\sum_{\alpha\beta}(Z_{i,\alpha\beta}^\star)^2. \tag{9}$$

When the unit cell has a a net charge Z, $Z^\star$ in Eq. (8) should be replaced by $Z^{\star\prime}$. The sums in Eq. (8) are the same to within 2% for all the defect structures, indicating similar summed squared magnitudes of effective charges. There is, however, a pronounced difference in the *spatial* variation of $Z^\star$, as shown in Fig. 6, in which the Hf $Z_i^\star=+\sqrt{(Z_i^\star)^2}$ have been plotted. Note that the Hf $Z^\star$ are substantially reduced near the vacancy. Near the defect, $Z^\star$ is more reduced for the

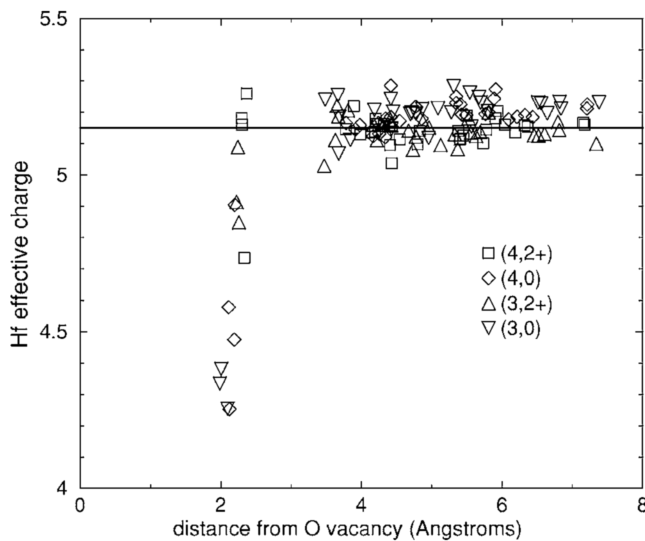

FIG. 6. Born effective charge of Hf vs distance from the defect center. The $Z^{\star}$ for Hf in defect-free HfO_2 is indicated by the solid horizontal line.

neutral vacancy than for the charged vacancies. On the other hand, away from the defect, $Z^{\star}$ is larger for the neutral vacancies. Among the Hf nearest the defect, the reduction in $Z^{\star}$ is concentrated on a specific Hf ion $(4,2+)$ or pair of ions $(3,2+)$ when the vacancy is charged. This indicates a more asymmetric relaxation around a charged vacancy than around a neutral vacancy. In all cases, the Hf effective charge becomes nearly equal to its bulk value for all Hf that are not adjacent to the vacancy.

V. CONCLUSIONS

Full dielectric tensors were calculated from first principles for monoclinic HfO_2 with and without oxygen vacancies. With one oxygen vacancy per 64 oxygen atoms, the static dielectric constant κ_s is increased by 1%–2% for neutral vacancies and suppressed by 1%–3% for 2+ charged vacancies. The increase in κ_s for neutral oxygen vacancies arises from an enhancement of the electronic dielectric response due to a pair of electrons occupying an easily polarizable defect state. The suppression in κ_s for charged oxygen vacancies is due to phonon hardening, which reduces the ionic response. No evidence is found that oxygen vacancies in HfO_2 introduce localized infrared- or Raman-active phonons whose characteristic frequency could be detected experimentally.

ACKNOWLEDGMENTS

I would like to thank Y. J. Chabal, J. Gavartin, M. Green, C. Hacker, E. J. Heilweil, P. Sushko, and D. Vanderbilt for helpful discussions.

[1] G. D. Wilk, R. M. Wallace, and J. M. Anthony, J. Appl. Phys. **89**, 5243 (2001).
[2] D. G. Schlom and J. H. Haeni, MRS Bull. **27**, 198 (2002).
[3] J. Robertson, Eur. Phys. J.: Appl. Phys. **28**, 265 (2004).
[4] S. Zafar, A. Callegari, E. Gusev, and M. V. Fishetti, J. Appl. Phys. **93**, 9298 (2003).
[5] H. S. Balk, M. Kim, G.-S. Park, S. A. Song, M. Varela, A. Franceschetti, S. T. Pantelides, and S. J. Pennycook, Appl. Phys. Lett. **85**, 672 (2004).
[6] A. S. Foster, F. Lopez Gejo, A. L. Shluger, and R. M. Nieminen, Phys. Rev. B **65**, 174117 (2002).
[7] J. L. Gavartin, A. L. Shluger, A. S. Foster, and G. I. Bersuker, J. Appl. Phys. **97**, 053704 (2005).
[8] N. Umezawa, K. Shiraishi, T. Ohno, H. Wantanabe, T. Chikyo, K. Torii, K. Yamabe, K. Yamada, H. Kitajima, and T. Arikado, Appl. Phys. Lett. **86**, 143507 (2005).
[9] K. Xiong, J. Robertson, M. C. Gibson, and S. J. Clark, Appl. Phys. Lett. **87**, 183505 (2005).
[10] J. Robertson, Rep. Prog. Phys. **69**, 327 (2006).
[11] J. Robertson, K. Xiong, and S. J. Clark, Phys. Status Solidi B **243**, 2054 (2006).
[12] J. L. Gavartin, D. M. Ramo, A. L. Shluger, G. Bersuker, and B. H. Lee, Appl. Phys. Lett. **89**, 082908 (2006).
[13] X. Zhao and D. Vanderbilt, Phys. Rev. B **65**, 233106 (2002).
[14] V. Fiorentini and G. Gulleri, Phys. Rev. Lett. **89**, 266101 (2002).
[15] G. M. Rignanese, X. Gonze, G. Jun, K. Cho, and A. Pasquarello, Phys. Rev. B **69**, 184301 (2004).
[16] G. Dutta, K. P. S. S. Hembram, G. M. Rao, and U. V. Waghmare, Appl. Phys. Lett. **89**, 202904 (2006).
[17] M. Born and K. Huang, *Dynamical Theory of Crystal Lattices* (Oxford University Press, Oxford, 1954).
[18] E. Cockayne and B. P. Burton, Phys. Rev. B **62**, 3735 (2000).
[19] J. Adam and M. D. Rodgers, Acta Crystallogr. **12**, 951 (1959).
[20] R. E. Hann, P. R. Suttch, and J. L. Pentecost, J. Am. Ceram. Soc. **68**, C285 (1985).
[21] G. Kresse and J. Furthmuller, Phys. Rev. B **54**, 11169 (1996).
[22] P. E. Blochl, Phys. Rev. B **50**, 17953 (1994).
[23] G. Kresse and D. Joubert, Phys. Rev. B **59**, 1758 (1999).
[24] A. B. Mukhopadhyay, J. F. Sanz, and C. B. Musgrave, Phys. Rev. B **73**, 115330 (2006).
[25] X. Gonze, J.-M. Beuken, R. Caracas, F. Detraux, M. Fuchs, G.-M. Rignanese, L. Sindic, M. Verstraete, G. Zerah, F. Jollet *et al.*, Comput. Mater. Sci. **25**, 478 (2002).
[26] C. Hartwigsen, S. Goedecker, and J. Hutter, Phys. Rev. B **58**, 3641 (1998).
[27] S. Baroni, S. de Gironcoli, A. D. Corso, and P. Giannozzi, Rev. Mod. Phys. **73**, 515 (2001).
[28] M. Leslie and M. J. Gillan, J. Phys. C **18**, 973 (1985).
[29] O. Zakharov and M. L. Cohen, Phys. Rev. B **52**, 12572 (1995).
[30] R. D. King-Smith and D. Vanderbilt, Phys. Rev. B **47**, 1651 (1993).
[31] R. Resta, Rev. Mod. Phys. **66**, 899 (1994).
[32] M. Balog, M. Shieber, M. Michiman, and S. Patai, Thin Solid Films **41**, 247 (1977).
[33] B.-K. Kim and H. Hamaguchi, Mater. Res. Bull. **32**, 1367 (1997).
[34] D. A. Neumayer and E. Cartier, J. Appl. Phys. **90**, 1801 (2001).

[35] C. A. Hacker and E. J. Heilweil (unpublished).
[36] R. A. B. Devine, Appl. Phys. Lett. **68**, 3108 (1996).
[37] K. T. Queeney, M. K. Weldon, J. P. Chang, Y. J. Chabal, A. B. Gurevich, J. Sapjeta, and R. L. Opila, J. Appl. Phys. **87**, 1322 (2000).
[38] M. M. Frank, S. Sayan, S. Dörmann, T. J. Emge, L. S. Wielunski, E. Garfunkel, and Y. J. Chabal, Mater. Sci. Eng., B **109**, 6 (2004).
[39] N. V. Nguyen, A. V. Davydov, D. Chandler-Horowitz, and M. M. Frank, Appl. Phys. Lett. **87**, 192903 (2005).
[40] G.-M. Rignanese, J. Phys.: Condens. Matter **17**, R357 (2005).
[41] J. D. Jackson, *Classical Electrodynamics*, 2nd ed. (Wiley, New York, 1975).